Catalyst deactivation of a silica-supported bismuth-molybdenum complex oxide and the related complex oxides for the oxidative dehydrogenation of 1-butene to 1,3-butadiene

Shigeru SUGIYAMA[1,2*], Kohta NAGAI[3], Yuki NAKAO[3], Yuzo BABA[1], Masahiro KATOH[1]

[1]*Department of Applied Chemistry, Graduate School of Science and Technology, Tokushima University, Minamijosanjima, Tokushima-shi, Tokushima 770-8506, Japan*

[2]*Department of Resource Circulation Engineering, Center for Frontier Research of Engineering, Tokushima University, Minamijosanjima, Tokushima-shi, Tokushima 770-8506, Japan*

[3]*Department of Chemical Science and Technology, Tokushima University, Minamijosanjima, Tokushima-shi, Tokushima 770-8506, Japan*

Keywords: Catalyst deactivation, Bismuth-molybdenum oxide, Oxidative dehydrogenation, 1-Butene, 1,3-Butadiene

Abstract

This study was an examination of the catalyst deactivation of a silica-supported bismuth-molybdenum complex oxide, and that of catalysts used in the absence of bismuth, for the oxidative dehydrogenation of 1-butene. Due to the detection of deactivation, the molar ratio of 1-butene against oxygen in the reactant gas was adjusted to a ratio similar to that used in industrial processes where reaction temperatures average 100 K higher. Regardless of the presence or absence of bismuth in the catalysts, the conversion of 1-butene was decreased by 6 h on-stream. Both the progress of the coking from the inlet to the outlet of the catalyst and the reduction of molybdenum in the catalysts directly contributed to the deactivation. X-ray photoelectron spectrometry revealed that a greater reduction of molybdenum in the near-surface region and a smaller partial pressure of oxygen ($P(O_2)$) in the reactant gas, although the molybdenum on the surface was not reduced at all. This indicated that the lattice oxygen was pumped from the near-surface region to the surface during the reaction and the oxygen-poor conditions of the near-surface region both in the gas and catalyst phases were formed at a smaller $P(O_2)$, which resulted in the enhancements of both the reduction of molybdenum and that of coking. Based on the thermogravimetric analysis, the silica-supported bismuth-molybdenum complex oxide used at $P(O_2)$ = 4.1 kPa (color of the catalyst = black) was increased in weight while that used at $P(O_2)$ = 16.4 kPa (color of the catalyst = gray) showed a weight decrease, which indicated that the weight decrease caused by the reduction in molybdenum in the near-surface region used at 4.1 kPa was greater than the weight increase from the coking. It was concluded that the reduction in molybdenum followed by the coking on the catalyst surface were the main factors in the catalyst deactivation.

Introduction

Bismuth-molybdenum complex oxide catalysts (SOHIO process) were first used in the 1960s (Grasselli and Burrington, 1981; Moro-oka and Ueda, 1994) to produce acrylonitrile via the ammoxidation of propylene, and this system has been a key industry oxidative catalyst for this reaction (Burrington and Gresselli, 1979) and others including the production of acrylic acid via the oxidation of propylene (Anderson *et al*., 1985), that of methacrolein via the oxidation of isobutene (Voge and Adams, 1967), and so on. More recently, this catalyst system has been adapted to the synthesis of 1,3-butadiene from butenes via oxidative dehydrogenation (Matsuura *et al*., 1980; Soares *et al*., 2003; Jung *et al*., 2008) since 1,3-butadiene is a fundamental chemical precursor for the production of styrene-butadiene rubber, polybutadiene rubber, and advanced polymers such as acrylonitrile-butadiene-styrene resin (ABS resin). Since bismuth-molybdenum complex oxide catalysts are used extensively in many processes, aspects such as the mechanism, the additive effects, etc., continue to be studied (Park *et al*., 2012; Zhai *et al*., 2015). Based on extensive study of bismuth-molybdenum complex oxide catalysts, doping with transition metals such as iron and cobalt has been used to enhance the catalytic activity, and the catalyst is now believed to consist of two phases: a catalytic active site for hydrogen-abstraction from the substrate on Bi centers in Bi-Mo-oxide; and, an oxygen-carrier phase of lattice oxygen in Mo-oxide doped with the previously mentioned transition metal elements (Moro-oka and Ueda, 1994; Grasselli, 2002) (**Figure 1**). It should be noted, however, that without exception a catalyst deactivation on bismuth-molybdenum complex oxide catalysts has become a serious problem in all processes. Since it is generally accepted that bismuth-molybdenum complex oxide catalysts are complete, only a few studies have focused on the deactivation of complex oxide catalysts. For example, a recent 48 h on-stream investigation into the oxidative dehydrogenation of C_4 raffinate-3 to 1,3-butadiene on bismuth molybdate catalysts showed stable activity during the reaction (Jung *et al*., 2007). However, it is generally accepted by

E-mail address of corresponding author: sugiyama@tokushima-u.ac.jp*

those concerned with the practical processes of catalytic reactions that there is an evident deactivation process that proceeds during operational periods lasting longer than year. This estrangement between academia and industry is, therefore, remarkable.

In the present study, bismuth-molybdenum complex oxide catalysts, as well as the corresponding oxygen carrier phase prepared during the procedure shown in some patents, were used in the oxidative dehydrogenation of 1-butene in order to trace the origin of the catalyst activation. In the present study, it was rather important to consider the reaction conditions since these results should be applicable to industrial processes. Therefore, the molar ratio of 1-butene against oxygen in the reactant gas was adjusted to a ratio similar to that commonly used in industrial processes. In order to more clearly detect the catalyst deactivation based on the scale used in the reaction, the reaction temperature was sat at 723 K, which was approximately 100 K higher than that used in an industrial process. As with industrial processes (Teshigahara *et al*., 2009; Kameo *et al*., 2012), a molybdenum-rich catalyst was used in the present study because the molybdenum in the complex oxide catalyst sublimates at reaction temperatures higher than 673 K (Tanimoto, 2003). Furthermore, the presence of a rich molybdenum oxide resulted in an enhanced mobility of the lattice oxygen in the oxygen carrier phase (Moro-oka and Ueda, 1994) along with the formation of coking (Kameo *et al*., 2012). Therefore, in order to clarify the cause of the catalytic deactivation, the oxidative dehydrogenation of 1-butene was examined for four types of oxygen carrier phases; molybdenum excessive, rich, equivalent, and poor.

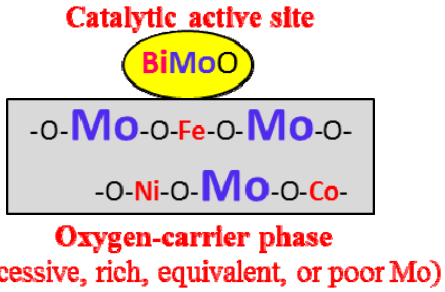

Fig. 1 Concept of bismuth-molybdenum complex oxide catalysts

1. Experimental

According to the preparation procedure of a silica-supported bismuth-molybdenum complex oxide catalyst (Teshigahara et al., 2009; Kameo et al., 2012), one catalyst (Catalyst 1) with a rich molybdenum and four oxygen carrier phases were prepared: Carriers 1, 2, 3, and 4, showing excessive, rich, equivalent, and poor molybdenum phases, respectively, calculated for MoO_3, Fe_2O_3, CoO, and NiO, while bismuth was absent. The compositions of those materials are listed in Table 1. As shown in the patents, those materials also contained cobalt, nickel, and iron to enhance the mobility of the lattice oxygen in a catalyst (Teshigahara et al., 2009; Kameo et al., 2012).

Table 1 Atomic ratios in the catalyst and oxygen carrier phases.

	Mo	Bi	Co	Ni	Fe	Si
Catalyst 1	12.0	5.0	1.7	1.7	0.4	24.0
Carrier 1	6.9	-	1.7	1.7	0.4	24.0
Carrier 2	4.0	-	1.7	1.7	0.4	24.0
Carrier 3	3.8	-	1.7	1.7	0.4	24.0
Carrier 4	3.6	-	1.7	1.7	0.4	24.6

The catalyst and oxygen carrier phases were analyzed via X-ray diffraction (XRD; RINT 2500X, Rigaku Co.) and nitrogen adsorption-desorption measurement (BELSORP-max12, Bel Japan Inc.). The powder XRD patterns of the materials were obtained using monochromatized Cu Kα radiation (40 kV, 40 mA). Before the nitrogen adsorption-desorption measurement at 77 K, the catalysts were pretreated at 473 K for 5 h under vacuum. The BET surface area was calculated from an obtained isotherm. The surface properties on the materials were evaluated via X-ray photoelectron spectroscopy (XPS; PHI-5000VersaProbe II, ULVAC-PHI Inc.). The XPS spectra of the catalysts were calibrated based on a C 1s peak at 285.0 eV. Thermogravimetric analysis (TG) was carried out using a TG/DTA 6300 apparatus (SII Nanotechnology Inc.) with a heating rate of 5 ℃/min under flowing air (100 mL/min).

The catalytic activity tests were carried out in a fixed-bed continuous-flow reactor at atmospheric pressure (Ehiro *et al*., 2016). Each catalyst (0.5 g) was pelletized and sieved to 0.85–1.70 mm. They were fixed with quartz wool and pretreated with 25 mL/min of O_2 gas flow at 723 K for 1 h. After the pretreatment, catalytic activity tests were started at 723 K by flowing 30 mL/min of a gas mixture of helium, 1-butene and oxygen to the reactor. Their partial pressures were adjusted to $P(1\text{-}C_4H_8)$ = 14.4 kPa, and $P(O_2)$ = 4.1, 8.2 or 16.4 kPa, and diluted with He. The combination of $P(1\text{-}C_4H_8)$ = 14.4 kPa and $P(O_2)$ = 16.4 kPa corresponded to the range used in an industrial process (Teshigahara et al., 2009; Kameo et al., 2012). A temperature controller was used to maintain the reaction temperature to a constant level (AMF-1P, Ikemoto Scientific Technology Co., Ltd.). Under these conditions, a homogeneous gas phase reaction was not observed. The reaction was monitored using both a gas chromatograph (GC-8APT, Shimadzu Corp.) equipped with a TCD and a capillary gas chromatograph (GC-2025, Shimadzu Corp.) equipped with a FID. For the former, a Molecular Sieve 5A (MS 5A, 0.2 m×Φ3 mm) for O_2, CH_4 and CO and a Porapak Q (3.0 m×Φ3 mm) for CO_2 were used as the columns at 318 K. For the

latter, Rt@-Alumina BOND/Na_2SO_4 capillary column (Restek Co., 30 m × Φ 0.53 mm) was used for C_2, C_3 and C_4 species at 403 K. The carbon balance between the reactant and the products was within ±5%. Both product selectivity and 1-butene conversion were calculated on a carbon basis.

2. Results and Discussion

2.1 Deactivation behaviors of a silica-supported bismuth-molybdenum complex oxide catalyst

Figure 2 shows the effects of the partial pressure of oxygen ($P(O_2)$ = 4.1, 8.2 and 16.4 kPa) for the oxidative dehydrogenation of 1-butene on Catalyst 1 at 0.75 and 6 h on-stream. The conversions of 1-butene from 0.75 to 6 h on-stream at $P(O_2)$ = 4.1, 8.2 and 16.4 kPa were shifted from 69.4 to 63.8%, from 75.5 to 72.9%, and from 89.2 to 89.5%, respectively, indicating that the catalyst deactivation proceeded more clearly at a lower $P(O_2)$. This deactivation affected the selectivity to 1,3-butadiene: $P(O_2)$ = 4.1, 8.2 and 16.4 kPa from 79.6 to 83.6%, from 77.1 to 79.7% and from 57.5 to 59.8%, respectively. Therefore, a higher $P(O_2)$ resulted in stable activity during 6 h on-stream while the deep oxidation of 1,3-butadiene to COx proceeded. In contrast, a lower $P(O_2)$ resulted in the evident deactivation while the deep oxidation was suppressed.

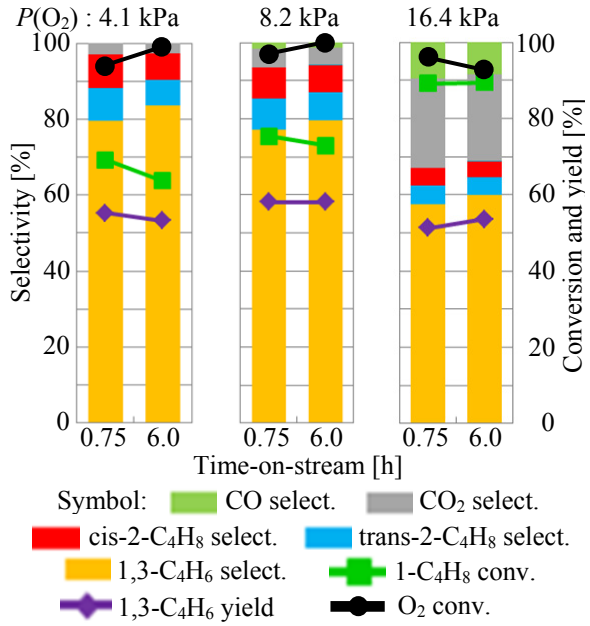

Fig. 2 Catalytic activity on Catalyst 1 at various partial pressures of oxygen.

The color change of Catalyst 1 after the reaction is shown in **Figure 3**. The color of Catalyst 1 was changed from white to black and gray after the reaction at $P(O_2)$ = 4.1 and 16.4 kPa, respectively (**Figures 3 (a) and (b)**), indicating that coking had evidently occurred at the lower partial pressure, as expected, which resulted in an evident catalytic deactivation, as shown in Figure 2. Although the color of Catalyst 1 was completely changed to black, it should be noted that the color change of Catalyst 1 used at $P(O_2)$ = 16.4 kPa was evident in the outlet of the catalyst bed, while it appeared white in the inlet (**Figure 3 (c)**). This suggested that the oxygen-rich conditions in the inlet had maintained the catalyst in a fresh state, while oxygen-poor conditions in the outlet had resulted in the formation of coke.

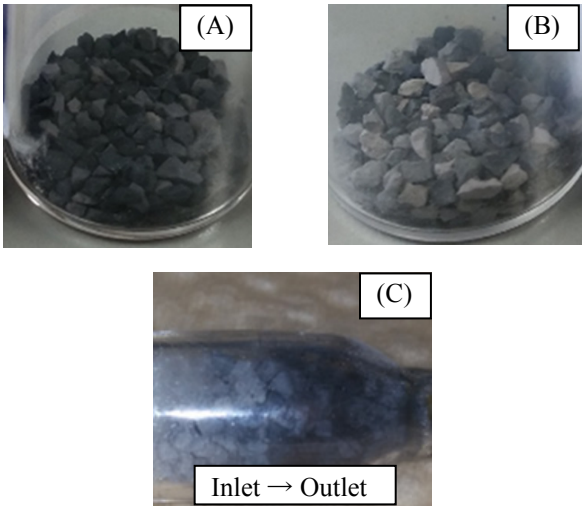

Fig. 3 Color change of Catalyst 1 used at $P(O_2)$ = 4.1 (A), 16.4 kPa (B) and view of the reactor charged with Catalyst 1 used at $P(O_2)$ = 16.4 kPa (C).

After Catalyst 1 (1 g) was used for the oxidative dehydrogenation of 1-butene at $P(1\text{-}C_4H_8)$ = 14.4 kPa and $P(O_2)$ = 16.4 kPa, F = 60 mL/min, and 723 K, the catalyst was divided into two sections, an inlet and an outlet (each 0.5 g). Those two sections were again used for oxidative dehydrogenation under the same conditions shown in Fig. 1, albeit with $P(O_2)$ = 16.4 kPa, and the results were compared with the activity of the fresh Catalyst 1 (**Figure 4**). It was evident that the results for the conversion of 1-butene and the yield of 1,3-butadine using fresh Catalyst 1 were similar to those at the outlet port of Catalyst 1 previously used in the oxidative dehydrogenation at P(O2) = 16.4 kPa, while those at the inlet port of Catalyst 1 were lower than those using fresh Catalyst 1. These results also indicate that oxygen-rich conditions in the inlet part resulted in the maintenance of fresh catalyst. By contrast, oxygen-poor conditions resulted in the formation of coke over the catalyst surface, which led to catalyst deactivation.

Figure 5 shows the XRD patterns of Catalyst 1 before and after the oxidative dehydrogenation of 1-butene at various levels of partial pressure for oxygen. Before the reaction, the XRD patterns due to $CoMoO_4$ (PDF 00-021-0868) and α-$Bi_2Mo_3O_{12}$ (PDF 01-078-2420) were evident. Since small amounts of Co, Ni and Fe species were contained in Catalyst 1, small peaks were also detected in the XRD, but these were unidentified.

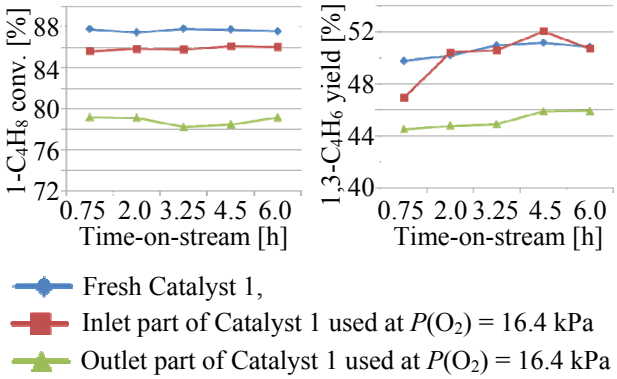

Fig. 4 Catalytic activity on fresh and used Catalyst 1 previously used for the oxidative dehydrogenation of 1-butene at $P(O_2)$ = 16.4 kPa.

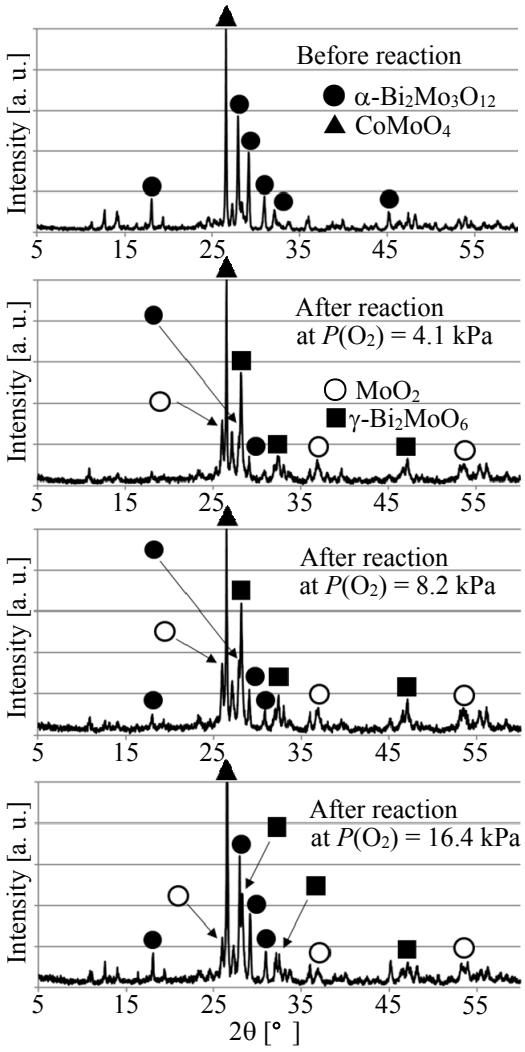

Fig. 5 XRD patterns of Catalyst 1 before and after the oxidative dehydrogenation of 1-butene at various partial pressures of oxygen.

It is generally accepted that α-$Bi_2Mo_3O_{12}$ together with γ-Bi_2MoO_6 is a catalytically active species for the oxidative dehydrogenation of 1-butene to 1,3-butadiene (Jung et al., 2006). After use in oxidative dehydrogenation, the peak intensity due to α-$Bi_2Mo_3O_{12}$ was decreased while new peaks due to MoO_2 (PDF 01-072-4534) and γ-Bi_2MoO_6 (PDF 01-077-1246) were detected. It should be noted that the peaks due to α-$Bi_2Mo_3O_{12}$ were rather evident when Catalyst 1 was used at $P(O_2)$ = 16.4 kPa while those peaks were smallest when Catalyst 1 was used at $P(O_2)$ = 4.1 kPa. This may indicate that the active species, α-$Bi_2Mo_3O_{12}$, had disappeared during oxidative dehydrogenation, which resulted in evident deactivation under oxygen-poor conditions at $P(O_2)$ = 4.1 kPa. The detection of MoO_2 after the reaction showed that the reduction of Mo^{6+} to Mo^{4+} had also proceeded during the reaction.

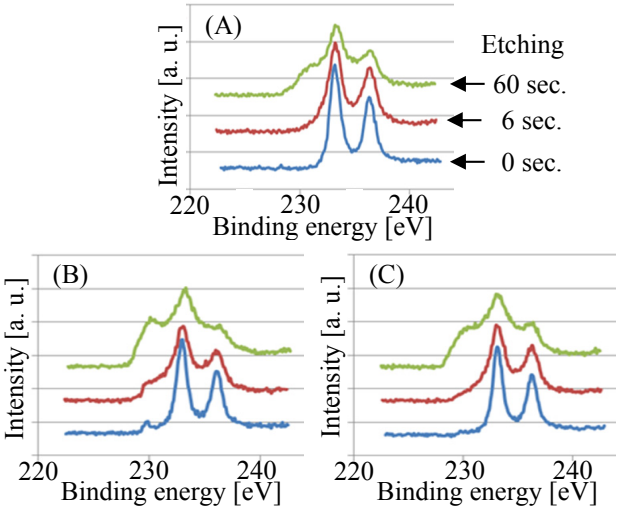

Fig. 6 XPS patterns of Catalyst 1 before (A) and after the oxidative dehydrogenation of 1-butene at $P(O_2)$ = 4.1 (B) and 16.4 kPa (C), respectively

Since the bulk structure of Catalyst 1 was strongly dependent on the partial pressure of oxygen in the reactant, XPS analysis, particularly on the Mo species, was also employed when examining its surface. As shown in **Figure 6 (A)**, two peaks due to $3d_{5/2}$ and $3d_{3/2}$ of Mo^{6+} were detected at 232.4 and 235.5 eV from the surface of fresh Catalyst 1 (Soares *et al.*, 2003). Similar peaks were also detected after 6 seconds of etching. Since it is generally accepted that α-$Bi_2Mo_3O_{12}$ and/or γ-Bi_2MoO_6 are catalytically active species in the oxidative dehydrogenation of 1-butene to 1,3-butadiene, Mo^{6+} should also be an active species for the reaction. After 60 seconds of etching, however, a shoulder was also detected at ca. 230 eV. It should be noted that two peaks due to $3d_{5/2}$ and $3d_{3/2}$ of Mo^{4+} were previously detected at ca. 230 and 233 eV (Soares *et al.*, 2003). Therefore, after 60 seconds of etching, the Mo^{4+} species was detected along with the Mo^{6+}species in fresh Catalyst 1. The presence of Mo^{4+} species was more evident from Catalyst 1 used at $P(O_2)$ = 4.1 kPa (**Figure 6 (B)**), where a small peak due to $3d_{5/2}$ of Mo^{4+} was detected on the surface of the catalyst. When Catalyst 1

was used at $P(O_2)$ = 16.4 kPa, however, Mo^{4+} did not appear on the surface of the catalyst (**Figure 6 (C)**).

These results indicate that the lattice oxygen in the catalyst moved from the bulk to the surface in order to maintain Mo^{6+} on the surface of the catalyst. Under oxygen-poor conditions during oxidative dehydrogenation, the reduction of Mo^{6+} to Mo^{4+} proceeded strongly. Therefore, the deactivation evident at $P(O_2)$ = 4.1 kPa shown in Figure 2 was reasonable due to the formation of Mo^{4+} on the catalyst surface, which resulted in deactivation particularly under such oxygen-poor conditions.

Based on the results shown above, coking and a reduction of Mo^{6+} to Mo^{4+} would be the main factors for catalyst deactivation on a silica-supported bismuth-molybdenum complex oxide catalyst. These results were further supported using the following TG analyses. As shown in **Figure 7**, the use of fresh Catalyst 1 resulted in a weight decrease due to absorbed water at ca. 473 K followed by a great loss at the temperatures higher than 873 K due to the sublimation of molybdenum oxide. Similar behavior was also observed from Catalyst 1 that had previously been used for the present reaction at $P(O_2)$ = 16.4 kPa due to a small amount of coking and the reduction of Mo^{6+} to Mo^{4+}. It should be noted that when Catalyst 1 was previously used for the present reaction at $P(O_2)$ = 4.1 kPa, the color was completely black, which indicated that coking had proceeded and was extensive. There was a weight increase, although it is generally accepted that the coking samples generally show a weight decrease in TG analysis. In this case, the Catalyst 1 used at $P(O_2)$ = 4.1 kPa suffered from a serious reduction during the present reaction, as shown in XPS for the near-surface region. Therefore, during TG analysis, the sample was oxidized and showed a weight increase, which indicated that the reduction had proceeded both on the near-surface region and also in the bulk phase — the oxygen carrier phase. TG behavior when using previously used Catalyst 1 for the present reaction at $P(O_2)$ = 8.2 kPa showed behavior that fell somewhere between those samples.

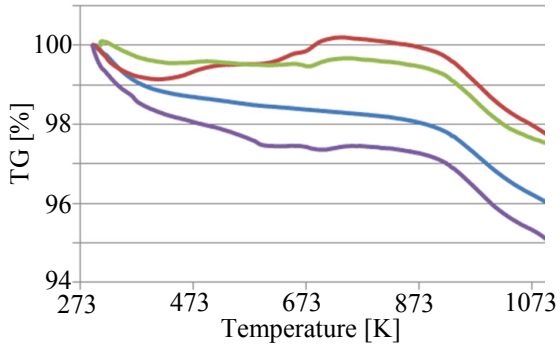

Fig. 7 TG curves of Catalyst 1 before (—) and after the oxidative dehydrogenation of 1-butene at $P(O_2)$ = 4.1 (—), 8.2 (—) and 16.4 kPa (—), respectively

It is generally accepted that the amount of coking can be estimated from the weight decrease in the TG behavior. However, the TG behavior in the present study was strongly influenced by the coking and the Mo-reduction during the reaction that was connected to the weight decrease and increase, respectively, during TG. Therefore, the extraction of only the weight decrease due to coking from the TG behavior was a difficult process.

2.2 Deactivation behaviors in the silica-supported oxygen-carrier phase

In order to examine the effect that reduction exerted on the oxygen carrier during the oxidative dehydrogenation of 1-butene, the reaction using Carrier 1 was performed at various levels of partial pressures.

As shown in **Figure 8**, regardless of the $P(O_2)$, the selectivity for 1,3-butadiene was lower than that when using Catalyst 1, which indicated that the oxidative dehydrogenation of 1-butene to 1,3-butadiene proceeded at the bismuth site of the catalyst. With a lower $P(O_2)$, the selectivities to cis-2-butene and trans-2-butene were enhanced while the selectivities to carbon monoxide and dioxide were enhanced at a higher $P(O_2)$. Since the isomerization of 1-butene to 2-butenes would proceed on the acidic site of a catalyst, the presence and absence of bismuth contributed to the selection of a suitable route to either oxidative dehydrogenation or isomerization. By contrast to the reaction with Catalyst 1 (Figure 2), regardless of the $P(O_2)$, catalyst deactivation was evident at those three values for $P(O_2)$, which indicated that the reduction of Catalyst 1 shown in Figure 2 was controlled by the combination of molybdenum and bismuth.

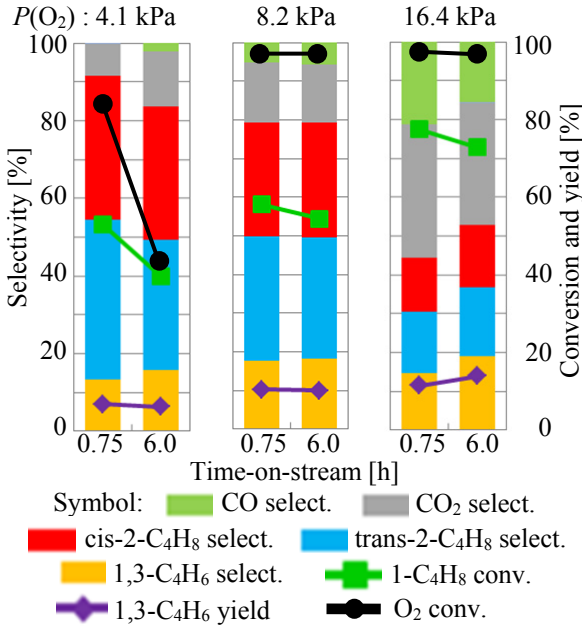

Fig. 8 Catalytic activity on Carrier 1 at various partial pressures of oxygen.

The same examination was carried out on Carriers 2, 3 and 4 at $P(O_2)$ = 4.1 kPa, and as shown in Figure 8, a similar tendency was obtained (**Figure 9**), indicating

that the catalyst deactivation in the oxygen carrier phase was only marginally influenced by the molybdenum content.

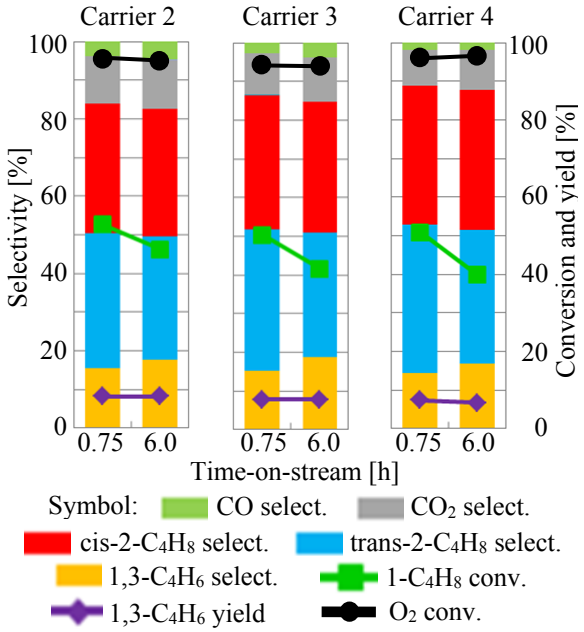

Fig. 9 Catalytic activity on Carrier 2, Carrier 3, and Carrier 4 at $P(O_2)$ = 4.1 kPa.

XRD analyses of fresh Carrier 1 showed that MoO_3 (PDF 01-076-1003) and $NiMoO_4$ (PDF 00-045-0142) were present as main components (**Figure 10**).

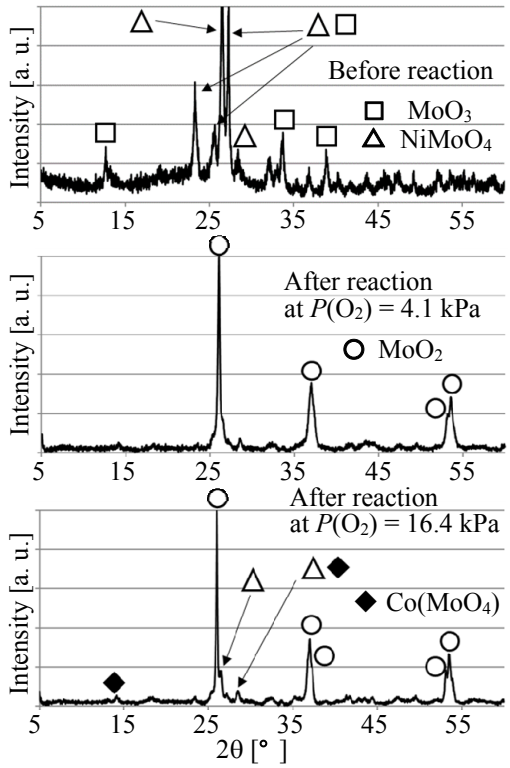

Fig. 10 XRD patterns of Carrier 1 before and after the oxidative dehydrogenation of 1-butene at various partial pressures of oxygen.

Following the reaction shown in Figure 8 at $P(O_2)$ = 4.1 and 16.4 kPa, XRD peaks due to both compounds had disappeared, while the intensity of the peaks due to MoO_2, together with that of the minor compound of $Co(MoO_4)$ (PDF 01-073-1331) was enhanced. Although the components in the fresh Catalyst 1 and those in Carrier 1 were dissimilar due to both the presence and absence, respectively, of bismuth, the reduction of Mo^{6+} to Mo^{4+} was similar from both following oxidative dehydrogenation. It should be noted that the presence of bismuth resulted in a suppression of the reduction during the reaction.

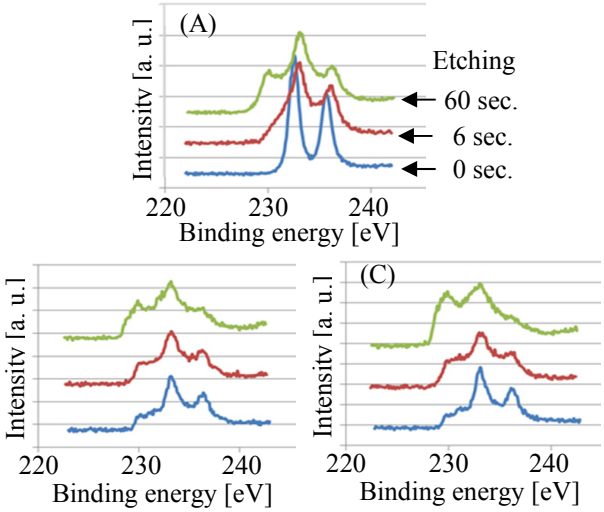

Fig. 11 XPS patterns of Carrier 1 before (A) and after the oxidative dehydrogenation of 1-butene at $P(O_2)$ = 4.1 (B) and 16.4 kPa (C), respectively

XPS analyses afforded more information on the reductive nature of molybdenum in the absence of bismuth. As shown in **Figure 11 (A)**, the surface nature of fresh Carrier 1 was essentially identical to that on fresh Catalyst 1 while the reduction in molybdenum was more evident after 60 seconds of etching from Carrier 1 than that from Catalyst 1 (Figure 6 (A)). It should be noted that a reduction in molybdenum was detected even on the surface of Carrier 1, which indicated that the reduction with Carrier 1 proceeded more favorably than that with Catalyst 1, which indicated that the molybdenum on Carrier 1 afforded the reduction more easily than Catalyst 1. Therefore, the catalyst deactivation shown in Figure 9 was detected from Carrier 1.

The effects that the partial pressure of the oxygen in the reactant gas exerted on the reduction and coking behaviors are shown in **Figure 12**. After using oxygen-poor conditions with a $P(O_2)$ = 4.1 kPa, Carrier 1 showed TG behaviors that differed from those previously used with two other values for partial pressures. Catalyst 1 showed (Figure 7) a weight increase at ca. 673 K. This also indicated that when Carrier 1 was used at $P(O_2)$ = 4.1 kPa, it also suffered from a serious reduction that led to a reduction in

molybdenum while the sample was re-oxidized to show the weight increase during TG analyses. Furthermore, an extreme weight decrease due to the elimination of coking was observed at temperatures higher than ca. 673 K. This evident weight decrease was not observed from Carrier 1 when it was used at $P(O_2)$ = 8.1 and 16.4 kPa. Therefore, Carrier 1 suffered from serious coking during the oxidative dehydrogenation of 1-butene, particularly at $P(O_2)$ = 4.1 kPa.

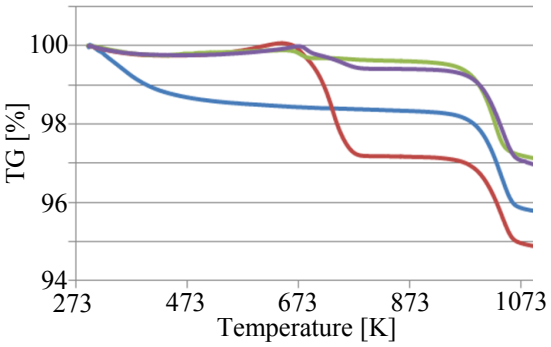

Fig. 12 TG curves of Carrier 1 before (—) and after the oxidative dehydrogenation of 1-butene at $P(O_2)$ = 4.1 (—), 8.2 (—) and 16.4 kPa (—), respectively

As mentioned above, the reduction in Mo species and coking were main factors for the catalyst deactivation. Furthermore the effect of the sublimation of molybdenum oxide has been pointed out as a factor for the deactivation. Based on Figures 7 and 12, the sublimation temperatures due to the molybdenum oxide seemed to be higher than 873 K. This temperature is lower than the present reaction temperature (723 K). Therefore the temperature may be low enough to suppress the sublimation. However, it should be noted that industrial processes suffer from confinement of the pipes due to molybdenum oxide sublimated from the catalyst in the corresponding industrial processes at 623 K (Teshigahara *et al*., 2009; Kameo *et al*., 2012). This indicates that the slight decrease in weight that started at approximately 400 K, as shown in Figures 7 and 12, may have contributed to the sublimation of molybdenum oxide. In this case, the catalyst previously used in the reaction will not be regenerated after the calcination in oxygen flow due to the lack of molybdenum oxide. In order confirm the present problem, the Catalyst 1 previously used in the catalytic reaction at $P(O_2)$ = 4.1 kPa (Figure 5) was calcined for 1 h at 723 K under an oxygen flow (30 mL/min) to be analyzed via XRD. In **Figure 13**, the XRD of Catalyst 1 before the reaction (before the reaction in Figure 5), and that after the calcination of the Catalyst 1 previously used for the reaction (Figures 2 and 5 at $P(O_2)$ = 4.1 kPa) were compared. It was evident that the intensity due to α-$Bi_2Mo_3O_{12}$ in the calcined Catalyst 1 was weaker than fresh α-$Bi_2Mo_3O_{12}$. It should be noted that the reaction during 6 h on-stream resulted in an evident difference in XRD for a catalyst that is customarily used in the corresponding industrial processes over a period of a year. This indicates that the sublimation of molybdenum oxide represents a serious problem in catalyst deactivation during the corresponding industrial processes.

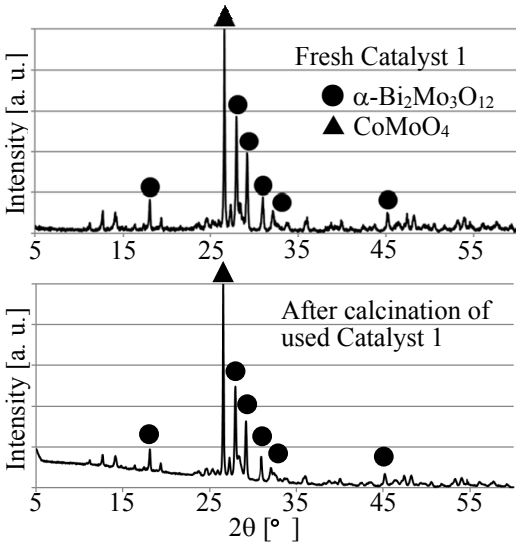

Fig. 13 XRD patterns of fresh Catalyst 1 and that after the calcination of Catalyst 1 previously used for the reaction at $P(O_2)$ = 4.1 kPa

Conclusions

Catalyst deactivation was detected on a silica-supported bismuth-molybdenum complex oxide catalyst, and a corresponding oxygen carrier was evident during the oxidative dehydrogenation of 1-butene when a much lower partial pressure of oxygen was used in the reactant gas. Since the reduction and coking during the reaction influenced the catalyst deactivation, sufficient oxygen supply into the feed-stream is required during oxidative dehydrogenation when using the present system.

Literature Cited

Anderson, A. B., D. W. Ewing, Y. Kim, R. K. Grasselli, J. D. Burrington and J. F. Brazdil; "Mechanism for Propylene Oxidation to Acrolein on $Bi_2Mo_3O_{12}$: A Quantum Chemical Study," *J. Catal*., **96**, 222-233 (1985)

Burrington, J. D. and R. K. Grasselli; "Aspects of Selective Oxidation and Ammoxidation Mechanisms over Bismuth Molybdate Catalysts," *J. Catal*., **59**, 79-90 (1979)

Ehiro, T., A. Itagaki, H. Misu, K. Nakagawa, M. Katoh, Y. Katou, W. Ninomiya and S. Sugiyama; "Effects of Acid Treatment on the Acidic Properties and Catalytic Activity of MCM-41 for the Oxidative Dehydrogenation of Isobutane," *J. Chem. Eng. Japan*, **49**, 152–160 (2016)

Grasselli, R. K.; "Fundamental Principles of Selective Heterogeneous Oxidation catalysis," *Catal. Lett*., **21**, 79-88 (2002)

Grasselli, R. K. and J. D. Burrington; "Selective Oxidation and Ammoxidation of Propylene by Heterogeneous Catalysis," *Adv. Catal.*, **30**, 133-163 (1981)

Kamei, H., H. Kajitani, K. Iwakai, H. Takeuchi, S. Orita and T. Takeuchi; "Conjugated Diene Production Method," International Publication No. WO 2012/121300 A1 (2012)

Jung, J. C., H. Kim, A. S. Choi, Y.-M. Chung, T. J. Kim, S. J. Lee, S.-H. Oh and I. K. Song; "Preparation, Characterization, and Catalytic Activity of Bismuth Molybdate Catalysts for the Oxidative Dehydrogenation of n-Butene into 1,3-Butadiene," *J. Mol. Catal. A: Chem*., **259**, 166-170 (2006)

Jung, J. C., H. Kim, Y. S. Kim, Y.-M. Chung, T. J. Kim, S. J. Lee, S.-H. Oh and I. K. Song; "Catalytic Performance of Bismuth Molybdate Catalysts in the Oxidative Dehydrogenation of C_4 Raffinate-3 to 1,3-Butadiene," Appl. Catal. A: Chem., 317, 244-249 (2007)

Jung, J. C., H. Lee, H. Kim, Y.-M. Chung, T. J. Kim, S. J. Lee, S.-H. Oh, Y. S. Kim and I. K. Song; "Effect of Oxygen Capacity and Oxygen Mobility of Pure Bismuth Molybdate and Multicomponent Bismuth Molybdate on their Catalytic Performance in the Oxidative Dehydrogenation of n-Butene to 1,3-Butadiene," *Catal. Lett.*, **124**, 262-267 (2008)

Matsuura, I., R. Schut and K. Hirakawa; "The Surface Structure of the Active Bismuth Molybdate Catalyst," *J. Catal*., **63**, 152-166 (1980)

Moro-oka, Y. and W. Ueda; "Multicomponent Bismuth Molybdate Catalyst: A Highly Functionalized Catalyst System for the Selective Oxidation of Olefin," *Adv. Catal*., **40**, 233-273 (1994)

Park J.-H., H. Noh, J. W. Park, K. Row, K. D. Jung and C.-H. Shin; "Effects of Iron Content on Bismuth Molybdate for the Oxidative Dehydrogenation of n-Butenes to 1,3-Butadiene," *Appl. Catal. A: Gen.,* **431-432**, 137-143 (2012)

Soares, A. P. V., L. D. Dimitrov, M. C.-R. A. de Oliveira, L. Hilaire, M. F. Portela and R. K. Grasselli; "Synergy Effects between β and γ Phases of Bismuth Molybdates in the Selective Catalytic Oxidation of 1-Butene," *Appl. Catal. A: Gen*., **253**, 191-200 (2003)

Tanimoto, M.; "Catalyst Technology in Acrylic Acid," *Catal. Catal.*, **45**, 360-365 (2003)

Teshigahara, T., N. Kanuka and T. Iwakura; "Production Method of Complex Oxide Catalyst," Japanese Patent No. 4280797 (2009)

Voga, H. H., and C. R. Adams; "Catalytic Oxidation of Olefins," *Adv. Catal*., **17**, 151-221 (1967)

Zhai, Z., X. Wang, R. Licht and A. T. Bell; "Selective Oxidation and Oxidative Dehydrogenation of Hydrocarbons on Bismuth Vanadium Molybdenum Oxide," *J. Catal*., **325**, 87-100 (2015)